Desalination and Water Treatment
www.deswater.com
doi: 10.1080/19443994.2015.1088897

57 (2016) 18417–18424
August

Taylor & Francis
Taylor & Francis Group

Selective sorption of Pb(II) from aqueous solution using an imprinted silica-supported sorbent based on the solgel imprinting technique

Yuanwei Liu

Department of Chemical Engineering, Binzhou University, Binzhou 256603, China, Tel. +86 13954388660; email: hbgfz@163.com

Received 14 December 2014; Accepted 26 August 2015

ABSTRACT

A lead ion-imprinted silica-supported sorbent (LIS) was prepared by the solgel method with lead ions as the template. The structural characteristics of the LIS were determined using Fourier transform infrared spectrometry and measurements of specific surface area. The selective adsorption performance of the LIS for the removal of Pb(II) from an aqueous solution was investigated in batch-type experiments. The adsorbent capacity and selectivity of the LIS were greater than those of the tested non-imprinted sorbent (NIS). The selectivity coefficients ($\alpha(K_{di}/K_{dj})$) of the LIS for Pb(II)/Cd(II) and Pb(II)/Ni(II) were 16.98 and 37.71, respectively, while those of NIS were only 3.53 and 3.29, respectively. Adsorption of Pb(II) by the LIS was well fitted by pseudo-second-order kinetic and Langmuir models. In addition, the thermodynamic parameters showed that Pb(II) adsorption onto the imprinted silica-supported LIS was an endothermic, positively entropic, and spontaneous sorption process.

Keywords: Selective adsorption; Pb(II); Imprinted silica-supported sorbent; Thermodynamics; Kinetic model

1. Introduction

Hazards associated with heavy metal ions are a prominent issue of concern worldwide, because such ions are widely distributed as environmental pollutants and threaten the quality of life of humans and other species [1]. The main methods for removing heavy metals from water include ion-exchange flocculation [2], reverse osmosis, chemical precipitation [3], extraction [4,5], membrane filtration [6], and adsorption [7]. Of the traditional techniques for removing heavy metals from water, adsorption is among the most widely used and most practical methods, because it is relatively environmentally friendly, low-cost [8].

Ion imprinting is a versatile technique that can be used to create materials that selectively recognize certain metal ion in the presence of a complex of the given metal ion. Ion-imprinted sorbents can be synthesized using ion templates. When the template metal ion is removed, a specific recognition site with an ionic radius very similar to that of the template ion is formed, producing a sorbent with selective adsorption capacity. Therefore, ion-imprinting technology has been used widely to produce sorbents intended for selective preconcentration, separation, or removal of particular ions [9–13].

The solgel manufacturing technique produces sorbents with several advantages over those produced

using other production methods, including high selectivity, high metal adsorption capacity, and excellent metal ion transfer kinetics [14–16]. The manufacture of Pb(II)-imprinted sorbents with the solgel process has been reported, but the authors used nano-silicon dioxide chemical modification, an inconvenient procedure affected by many factors that must be controlled to produce consistent results. In addition, manufacturing sorbents with the solgel method via nano-silica dioxide chemical modification requires an extra modifier, further increasing the cost of the process. Therefore, sorbent production via the solgel method with nano-silicon dioxide chemical modification is not suitable for industrial applications. In this work, a novel Pb(II)-imprinted silica-supported sorbent capable of selective adsorption of Pb(II) from aqueous solutions was synthesized via the solgel process with tetraethyl orthosilicate (TEOS) as a precursor. The adsorption characteristics of the lead ion-imprinted sorbent (LIS) were studied in detail. The selectivity of the manufactured sorbent was evaluated by calculating its distribution coefficient ($K_d(q_e/C_e)$) and relative selectivity coefficients ($\alpha(K_{di}/K_{dj})$) for Cd(II) and Ni(II). The kinetic and thermodynamic behavior of the adsorption of Pb(II) ions onto the LIS was also assessed.

2. Materials and methods

2.1. Raw materials

The Pb(II) nitrate template was obtained from Tian Da Chemical Company (Tian Jing, China). The TEOS precursor was purchased from Kelon Fine Chemical Company (Cheng Du, China). HCl and NaOH were purchased from Tian Da Chemical Company (Tian Jing, China) and used without alteration. Standard solutions of Cd(II), Pb(II), and Ni(II) were obtained from Long Tian Science and Technology Ltd. (Beijing, China). All chemicals were of analytical grade and used without further purification.

2.2. Synthesis of Pb(II)-imprinted silica-supported sorbent

The LIS was synthesized using the solgel process. In the first step of the method, complexation was achieved by mixing 45 mL ethanol and 1 g $Pb(NO_3)_2$ in 25 mL ethyl orthosilicate, after which the resulting mixture was stirred at 55℃ for 6 h. A white powder was obtained by vacuum drying the stirred mixture for 17 h at 80℃. The Pb(II) template was removed from the powder by successive washing with 2 mol L^{-1} HNO_3. Finally, the product was exhaustively washed with deionized water and dried to a constant weight at 80℃. The blank, non-imprinted sorbent (NIS) was synthesized using the same protocol, but without the addition of $Pb(NO_3)_2$.

2.3. Sorbent characterization

The structural characteristics of the sorbent were evaluated by Fourier transform infrared spectrometry (FT-IR) and measurements of specific surface area (BET). FT-IR spectra were recorded with an FT-IR spectrophotometer (Thermo Scientific Nicolet 380, Thermo Fisher Scientific, Waltham, MA, USA) in the range of 400–4,000 cm^{-1}. The median diameter (D_{50}) of the sorbents was measured using a Bettersize 2000 Intelligent Laser Particle Size Analyzer (Bettersize, Liaoning, China). The surface features of the sorbents were characterized using a 3H-2000PS2 specific surface area analyzer (Beishide Instrument-S&T Co., Ltd, Beijing, China). The surface topography of the sorbents was characterized via transmission electron microscopy (SEM) analysis at 5.0 kV (Hitachi S4800 TEM, Hitachi, Ltd, Tokyo, Japan).

2.4. Adsorption experiments

Batch adsorption was tested in 100 mL flasks with shaking for 270 min at 298 ± 2 K. The initial concentration of Pb(II) ions was 500 mg L^{-1}. Unless otherwise specified, 0.1 g of each sorbent was added. After shaking, the supernatant was withdrawn and analyzed using atomic absorption instrument (TAS986, Beijing's General Instrument Co., Ltd). The uptake capacity q_e (mg g^{-1}) of Pb(II) ion adsorption was calculated using the following equation [17]:

$$q_e = \frac{(C_0 - C_e)V}{m} \tag{1}$$

where C_0 and C_e (mg L) are the initial and equilibrium Pb(II) ion concentrations, respectively, V is the volume of the solution, and m is the mass (g) of the sorbent.

2.5. Selective adsorption

To test the adsorption of heavy metal Pb(II) ions by the sorbent during exposure to mixed ion species, mixed solutions of $Pb(NO_3)_2$, $Cd(NO_3)_2$, and $Ni(NO_3)_2$ were prepared (0.5 g L^{-1}, pH 5.0), to which 0.1 g of the sorbent was added (to 50 mL of each solution at 25℃ for 15 h). The solutions were filtered, after which serial dilutions were performed to allow measurement of the Pb(II) concentration using an atomic absorption spectrophotometer, from which the amount of adsorbed Pb(II) was calculated.

2.6. Desorption and sorbent reuse

To improve the usage life of the sorbent and reduce its cost, we eluted Pb(II) from used sorbent using 2 mol L^{-1} HNO_3, after which the sorbent was used again for Pb(II) adsorption. Pb(II) adsorption was tested 6 consecutive times.

3. Results and discussion

3.1. Characterization of chemically modified sorbents

The FT-IR spectra of NIS and the LIS are shown in Fig. 1.

The FT-IR spectra of the LIS and NIS showed similar peak locations, but the wave numbers of the LIS peaks were shifted lower due to the presence of Pb(II) ions in the LIS polymer. The strong absorption peaks at 1,086.12 and 957.83 cm^{-1} corresponded to Si–O–Si and Si–OH, respectively. In addition, Si–OH and Si–O absorption bands were observed at 796.89 cm^{-1} (stretching vibration mode) and 460.84 cm^{-1} (bending vibration).

The surface area of the native SiO_2 particles (NIS) was 158.2061 m^2 g^{-1}, while that of the LIS was 505.5485 m^2 g^{-1}. The total pore volume of the NNS was 0.0771 mL g^{-1}, while that of the LIS was 0.3155 mL g^{-1}. The average pore diameter of the NNS was 1.95 nm, while that of the LIS was 2.50 nm. In comparison with the NNS sorbent, LIS exhibited greater adsorptive capacity due to its larger surface area and pore diameter.

Fig. 2 shows the features of LIS and NIS using scanning electron microscopy (SEM). The native SiO2 particles (NIS) surface (Fig. 2(a)) has good porosity and smooth surfaces, while the lead ion-imprinted sorbent (NIS) is rough as shown in Fig. 2(b), indicating significant improvement in specific surface area.

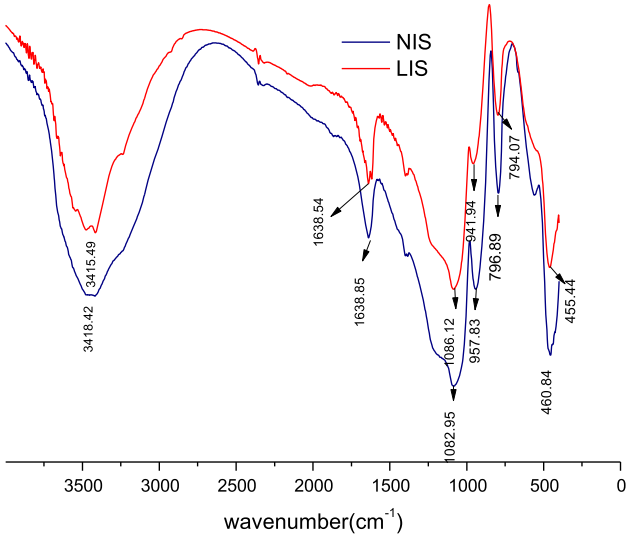

Fig. 1. FT-IR spectra of the LIS and NIS.

3.2. Selective adsorption assay

Cd(II) and Ni(II) ions were used to assess selective Pb(II) adsorption by the LIS (Table 1). The selective recognition ability of the LIS can be expressed using K_d and α, which can be calculated by the following equations:

$$K_d = q_e/C_e \tag{2}$$

where K_d is the distribution coefficient, q_e is the equilibrium adsorption capacity (mg g^{-1}), and C_e is the equilibrium concentration (mg L^{-1}), and

$$\alpha = K_{di}/K_{dj} \tag{3}$$

where α is the selectivity coefficient (the selective adsorption strength of the sorbents), i represents Pb (II), and j represents Cd(II) or Ni(II) ions. In the presence of Cd(II) and Ni(II) ions, the K_d value of the LIS for Pb(II) (101.7872) was higher than that of NIS (26.28588). Furthermore, the selectivity coefficients of the LIS for Pb(II)/Cd(II) and Pb(II)/Ni(II) were 16.98 and 37.71, respectively, while those of the NIS were 3.53 and 3.29. These results demonstrate that the LIS has greater selective adsorption ability for Pb(II) than the NIS, confirming that selective ion imprinting was achieved by the solgel synthesis.

3.3. Effect of the initial pH of the solution on Pb(II) sorption

The effect of the pH of the test solution on the Pb (II) adsorption capacity of the sorbents was studied over a pH range of 2.0–8.0, with all other parameters held constant. The relationship between adsorption capacity and pH is shown in Fig. 3. As pH was increased from 2.0 to 6.0, adsorption capacity increased rapidly to approximately 24 mg g^{-1}, at which it plateaued as the adsorption sites were saturated. The observed plateau in adsorption capacity may have been due to the decreasing concentration of H^+, which competed for Pb(II) binding, leading to conditions favorable for Pb(II) adsorption. Precipitation of indissoluble $Pb(OH)_2$ was more likely to occur above pH 7.0, while pH 6.0 was most favorable for Pb (II) adsorption.

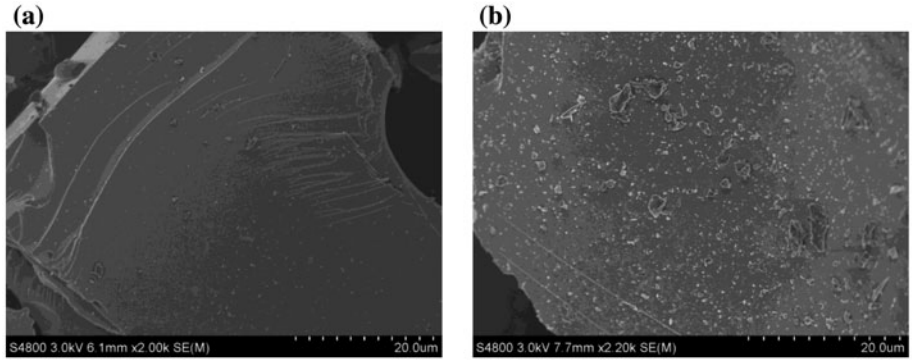

Fig. 2. SEM images of the lead ion-imprinted sorbent (NIS) and non-imprinted sorbent (LIS) (a) lead ion-imprinted sorbent (NIS) and (b) non-imprinted sorbent (LIS).

Table 1
Selective adsorption ability of the lead ion-imprinted sorbent (LIS) and the NIS

	NIS		LIS	
Substrate	K_d (mL g^{-1})	α	K_d (mL g^{-1})	α
Pb(II)	26.286	1	101.787	1
Cd(II)	7.4416	3.532	5.9934	16.984
Ni(II)	7.9736	3.297	2.699	37.7084

Note: K_d, distribution coefficient as calculated by Eq. (2).

3.4. Adsorption kinetics modeling

In order to determine the adsorption rate of the LIS and explore its mechanism of Pb(II) adsorption, Lagergren first-order and second-order kinetic models were applied. The following Lagergren first-order model equation was used [18,19]:

$$\ln(q_e - q_t) = \ln q_e - k_1 t \tag{4}$$

where q_e and q_t are the amounts of Pb(II) adsorbed (mg g^{-1}) at equilibrium and at time t, respectively, and k_1 is the rate constant (Fig. 4). The values of k_1 and q_e were calculated from the slope and intercept of the plots of $\log(q_e - q_t)$ vs. t.

The Lagergren second-order kinetic equation was as follows:

$$\frac{t}{q_t} = \frac{1}{k_2 q_e^2} + \frac{t}{q_e} \tag{5}$$

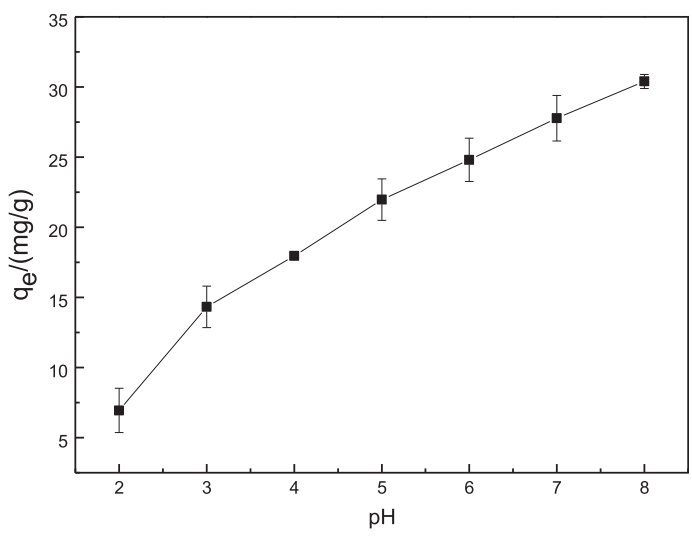

Fig. 3. Effect of initial solution pH on Pb(II) adsorption.

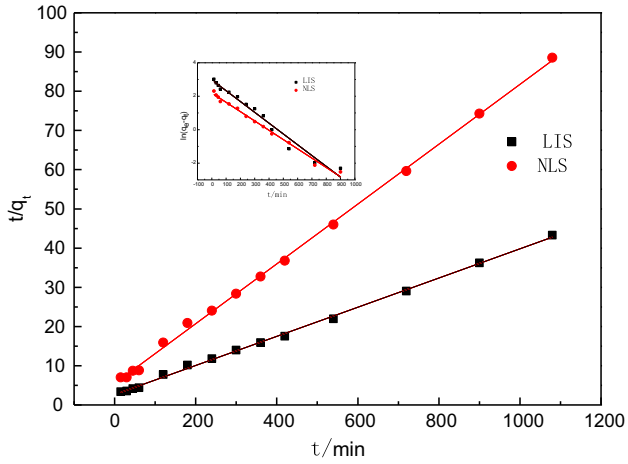

Fig. 4. Adsorption kinetics modeling.

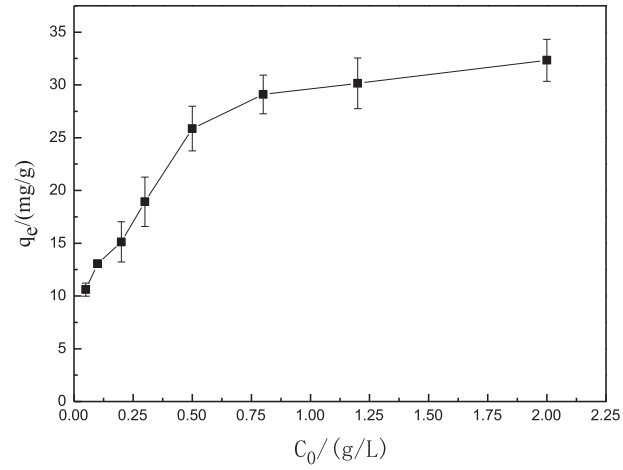

Fig. 5. Effect of the initial ion concentration on Pb(II) adsorption.

where k_2 (g mg^{-1} min^{-1}) is the equilibrium rate constant of the pseudo-second-order reaction. The value of k_2 was calculated from the slope and intercept of t/q_t vs. t (Table 2).

The kinetics data were fitted by the Lagergren first-order and second-order kinetics models (Fig. 4). The strong correlation between the models ($R^2 > 0.99$) showed that the pseudo-second-order model accurately represented the dynamics of the adsorption process, indicating a combination of physical and chemical adsorption of Pb(II) onto the adsorbent surface.

3.5. Adsorption equilibrium equation

The effect of the initial concentration of Pb(II) on adsorption was investigated with all other experimental conditions held constant (Fig. 5). The adsorptive capacity of the sorbents for Pb(II) increased as the initial ion concentration increased. At lower initial ion concentrations, adsorption increased rapidly due to the greater availability of binding sites for adsorption, whereas the adsorption capacity increased more slowly at higher initial ion concentrations because more adsorption sites were occupied by Pb(II).

The adsorption mechanism and surface behavior of the sorbent, which were both critical in the design of the separation process, were described by isotherm association. Langmuir and Freundlich isotherm models were fitted to the data (Fig. 6).

The Langmuir isotherm model indicated single-layer chemisorptive adsorption based on a homogeneous adsorbent surface, with the following linearized form [20]:

$$q_e = bq_m C_e/(1 + bC_e) \tag{6}$$

where q_e is the equilibrium adsorption capacity, C_e (mg L^{-1}) is the equilibrium concentration of Pb(II), and q_m is the maximum adsorption capacity.

The Freundlich isotherm model indicated multi-layer adsorption based on heterogeneous surfaces, with the following linearized form:

$$\ln q_e = \ln K_F + 1/n \ln C_e \tag{7}$$

where q_e (mg g^{-1}) is the absorption capacity, C_e (mg L^{-1}) is the equilibrium concentration of Pb(II),

Table 2
First- and second-order kinetic parameters for Pb(II) adsorption onto the tested sorbents

	First-order kinetic parameters			Exp. value	Second-order kinetic parameters		
	q_{em} (mg g^{-1})	k_1	R^2	q_m (mg g^{-1})	q_{em} (mg g^{-1})	k_2	R^2
R	25.425	0.00646	0.97303	24.94	25.246	0.03718	0.99787
I	12.18	0.00556	0.9898	12.2	117.786	−0.0190	0.99901

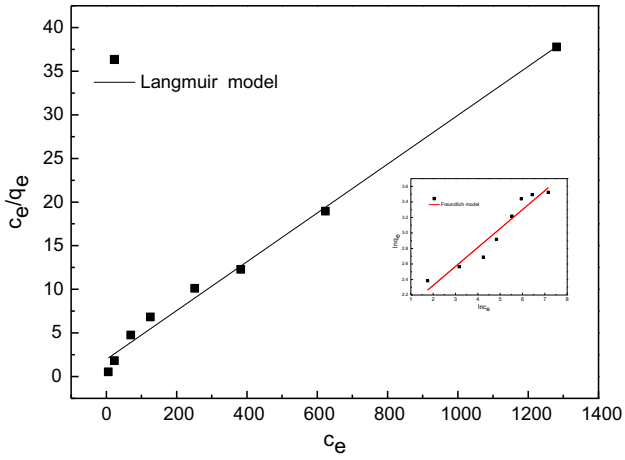

Fig. 6. Simulation of Pb(II) adsorption onto the LIS using the Langmuir and Freundlich models.

and K_F and $1/n$ are the Freundlich adsorption capacity and intensity, respectively.

The isotherm data were fitted with the Langmuir and Freundlich models (Table 3).

The experimental data fit the Langmuir isotherm model (R^2 = 0.99185) better than the Freundlich model (R^2 = 0.9216), indicating monolayer adsorption onto a heterogeneous surface. Moreover, the value of n (4.096) in the Freundlich model was between 1 and 10, indicating that Pb(II) was effectively adsorbed by the LIS [21]. The saturation adsorption capacity (35.72 mg g^{-1}) in the present work is higher than the values reported for Pb(II) adsorption on Pb(II)-IIP prepared by bulk polymerization (2.01 mg g^{-1}) [22], Pb(II)-imprinted amino-functionalized silica gel (19.66 mg g^{-1}) [23], and Pb(II)-IIP on nano-TiO2 matrix (22.70 mg g^{-1}) [24], respectively, while closes to imprinted polymer supported by SBA-15 (38.01 mg g^{-1}) [25].

3.6. Thermodynamic study

In order to reveal the isosteric heat of adsorption of the LIS, 3 adsorption thermodynamic conditions of Pb(II) from the best fitting isotherm were determined as follows [26,27]:

Table 3
Langmuir and Freundlich isotherm constants for Pb(II) adsorption onto the sorbents

	Langmuir			Freundlich		
	q_{em} (mg g^{-1})	b	R^2	K_F	n	R^2
R	35.727	0.0143	0. 99,185	6.273	4.096	0.9216

$$K = \lim \frac{q_{e\,mol}}{C_{e\,mol}} \tag{8}$$

$$\Delta G^0 = -RT \ln k_0 \tag{9}$$

$$\ln k = \Delta S^0/R - \Delta H^0/RT \tag{10}$$

$C_{e\ mol}$ (mol L^{-1}) and $q_{e\ mol}$ (mmol g^{-1}) corresponded to the equilibrium concentration of Pb(II) and the maximum adsorption capacity. K_0 is the equilibrium constant, while T and R are the temperature and gas constants, respectively. The enthalpy (ΔH) was determined from the slope of the plot of ln K_0 vs. $1/T$, as shown in Fig. 7.

The change in entropy (ΔS) was calculated using the following equation:

$$\Delta S = \frac{\Delta H - \Delta G}{T} \tag{11}$$

The effect of temperature on Pb(II) adsorption was studied at 25, 35, and 45℃. Three thermodynamic parameters were calculated (Table 4). The positive ΔH value showed that the adsorption process was endothermic and that Pb(II) was likely to adsorb at the highest tested temperature. The negative ΔG at various temperatures indicated that Pb(II) adsorption was endothermic and spontaneous, whereas the positive ΔS value indicated that adsorption contributed disorder.

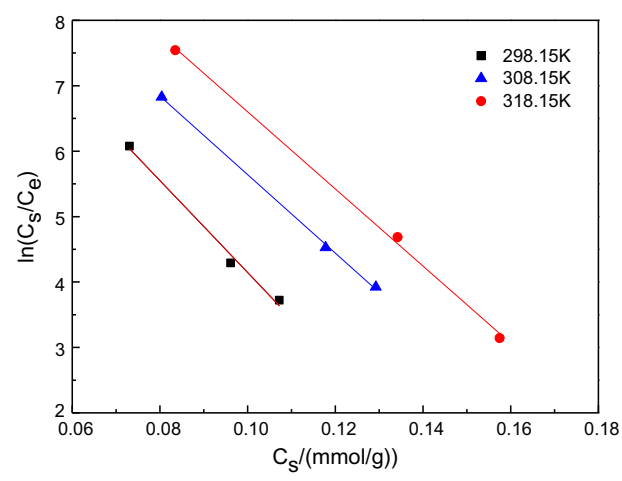

Fig. 7. Relationship between ln C_s/C_e and C_s at different temperatures.

Table 4
Thermodynamic parameters for Pb(II) adsorption onto the sorbents

ΔG (J mol^{-1})			ΔH	ΔS
298 K	308 K	318 K	(J mol^{-1} K^{-1})	(J mol^{-1} K^{-1})
−27.71	−29.82	−31.999	51.47	264.9

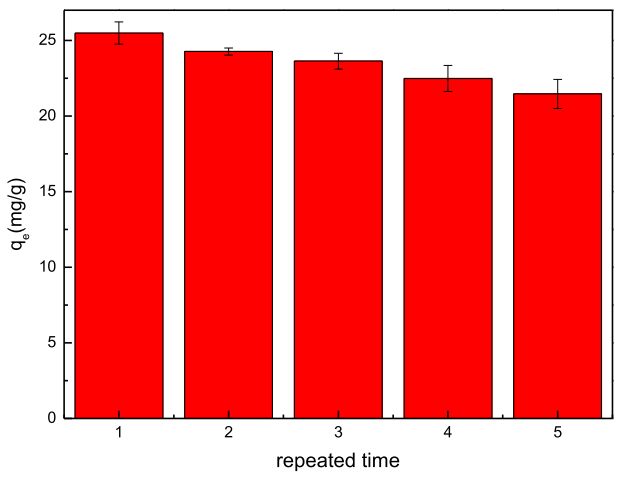

Fig. 8. Adsorptive capacity of repeated Pb(II) elution of LIS.

3.7. Desorption and reuse of the sorbent

To improve the usage life of the LIS and reduce its cost, we tested the potential of the LIS to be reused by repeatedly eluting the Pb(II) from the used sorbent and re-testing its absorptive capacity. The adsorptive capacity of the eluted sorbent is shown in Fig. 8. After 4 uses, the maximum adsorptive capacity of the sorbent was 88.5% of the initial capacity. These results demonstrate that the LIS can be used repeatedly as a Pb(II) adsorbent.

In Fig. 8, the bars represent the maximum adsorptive capacity of the imprinted sorbent for Pb(II) on successive tests following repeated elution of Pb(II) by HNO_3.

4. Conclusion

In this study, an LIS was synthesized for selective Pb(II) adsorption by the solgel process and successfully characterized through FT-IR and BET. The characteristics of the manufactured LIS and the NIS (blank control adsorbent) differed. The maximum adsorptive capacity of the LIS was 35.727 mg g^{-1} at a Pb(II) concentration of 1 g L^{-1}. The adsorption of Pb (II)ions onto the LIS was fit well by a Langmuir model, revealing the presence of homogeneous binding sites, while the adsorption kinetics followed a pseudo-second-order model, suggesting the occurrence of both physical and chemical adsorption. The value of n (4.096) indicated that Pb(II) was effectively adsorbed onto the LIS. The thermodynamic parameters showed that the process of adsorption onto the LIS was endothermic, endothermic, and spontaneous. Moreover, the relative selectivity coefficients indicated that the LIS was selective for Pb(II) over Cd(II) and Ni (II). Taken together, our results demonstrate that the LIS described herein represents an adsorbent with the ability to selectively remove Pb(II) ions from aqueous solutions. Future studies will determine the suitability of the LIS as an adsorbent for Pb pollution in environmental repair applications.

Acknowledgments

This work was supported by the Scientific Research Award Foundation for Shandong Provincial (ZR2014EMQ007), the Science and Technology Development Program of Binzhou (2013ZC0702).

References

[1] A. Shahat, M.R. Awual, M.A. Khaleque,M.Z. Alam, M. Naushad, A.M. Sarwaruddin Chowdhury, Large-pore diameter nano-adsorbent and its application for rapid lead(II) detection and removal from aqueous media, Chem. Eng. J. 273 (2015) 286–295.
[2] Z. Wang, Y. Ma, X. Hao, W. Huang, G. Guan, A. Abudula, Enhancement of heavy metals removal efficiency from liquid wastes by using potential-triggered proton self-exchange effects, Electrochim. Acta 130 (2014) 40–45.
[3] F. Zhuang, R. Tan, W. Shen, X. Zhang, W. Xu, W. Song, Monodisperse magnetic hydroxyapatite/Fe_3O_4 microspheres for removal of lead(II) from aqueous solution, J. Alloys Compd. 637 (2015) 531–537.
[4] M. Petersková, C. Valderrama, O. Gibert, J.L. Cortina, Extraction of valuable metal ions (Cs, Rb, Li, U) from reverse osmosis concentrate using selective sorbents, Desalination 286 (2012) 316–323.
[5] T.K. Rout, D.K. Sengupta, L. Besra, Flocculation improves uptake of ^{90}Sr and ^{137}Cs from radioactive effluents, Int. J. Miner. Process. 79 (2006) 225–234.
[6] L. Lebrun, F. Vallée, B. Alexandre, Q.T. Nguyen, Preparation of chelating membranes to remove metal cations from aqueous solutions, Desalination 207 (2007) 9–23.
[7] M. Jansch, P. Stumpf, C. Graf, E. Rühl, R.H. Müller, Adsorption kinetics of plasma proteins on ultrasmall superparamagnetic iron oxide (USPIO) nanoparticles, Int. J. Pharm. 428 (2012) 125–133.
[8] AS. Singha and A Guleria, Utility of chemically modified agricultural waste okra biomass for removal of toxic heavy metal ions from aqueous solution, J. Food Agric. Environ. 8 (2015) 52–60.

[9] W. Peng, Z. Xie, G. Cheng, L. Shi, Y. Zhang, Amino-functionalized adsorbent prepared by means of Cu(II) imprinted method and its selective removal of copper from aqueous solutions, J. Hazard. Mater. 294 (2015) 9–16.
[10] C.R.T. Tarley, F.N. Andrade, H. Santana, D.A.M. Zaia, L.A. Beijo, M.G. Segatelli, Ion-imprinted polyvinylimidazole-silica hybrid copolymer for selective extraction of Pb(II): Characterization and metal adsorption kinetic and thermodynamic studies, React. Funct. Polym. 72 (2012) 83–91.
[11] H. Faghihian, S.N. Mirsattari, K. Asghari, Kinetics and thermodynamics of Cu(II) adsorption by imprinted salen-functionalized silica gel, Desalin. Water Treat. 52 (37–39) (2014) 7205–7217.
[12] M. Meng, J. Wan, J. He, Y. Yan, A new molecularly imprinted polymer prepared by surface imprinting technique for selective adsorption towards kaempferol, Polym. Bull. 68 (2012) 1039–1052.
[13] H. Fan, J. Liu, H. Yao, Z. Zhang, F. Yan, and W. Li, Ion Imprinted Silica-Supported Hybrid Sorbent with an Anchored Chelating Schi. Base for Selective Removal of Cadmium(II) Ions from Aqueous Media, Ind. Eng. Chem. Res. 12.53(1) (2013) 369–378.
[14] H. Fan, Q. Tang, Y. Sun, Z. Zhang, W. Li, Selective removal of antimony(III) from aqueous solution using antimony(III)-imprinted organic–inorganic hybrid sorbents by combination of surface imprinting technique with sol–gel process, Chem. Eng. J. 258 (2014) 146–156.
[15] H. Fan, X. Fan, J. Li, M. Guo, D. Zhang, F. Yan, T. Sun, Selective Removal of Arsenic(V) from Aqueous Solution Using A Surface-Ion-Imprinted Amine-Functionalized Silica Gel Sorbent, Ind. Eng. Chem. Res. 51 (2012) 5216–5223.
[16] H. Fan, X. Sun, W. Li, Sol-gel derived ion-imprinted silica-supported organic–inorganic hybrid sorbent for selective removal of lead(II) from aqueous solution, J. Sol–Gel Sci. Technol. 72 (2014) 144–155.
[17] S. Veli, B. Alyüz, S. Veli, B. Alÿuz, Adsorption of copper and zinc from aqueous solutions by using natural clay, J. Hazard. Mater. 149 (2007) 226–233.
[18] N. Ghasemi, P. Tamri, A. Khademi, N.S. Nezhad, S.R.W. Alwi, Linearized Equations of Pseudo Second-order Kinetic for the Adsorption of Pb(II) on Pistacia Atlantica Shells, IERI Proc. 5 (2013) 232–237.
[19] J.P. Chen, L. Wang, Characterization of metal adsorption kinetic properties in batch and fixed-bed reactors, Chemosphere 54 (2004) 397–404.
[20] K.K. Krishnani, X. Meng, C. Christodoulatos, V.M. Boddu, Biosorption mechanism of nine different heavy metals onto biomatrix from rice husk, J. Hazard. Mater. 153 (2008) 1222–1234.
[21] I. Vázquez, J. Rodríguez-Iglesias, E. Marañón, L. Castrilló, M. Álvarez, Removal of residual phenols from coke wastewater by adsorption, J. Hazard. Mater. 147 (2007) 395–400.
[22] C. Esen, M. Andac, N. Bereli, R. Say, E. Henden, A. Denizli,Highly selective ion-imprinted particles for solid-phase extraction of Pb^{2+} ions, Mater. Sci. Eng. C 29(2009) 2464–2470.
[23] X. Zhu, Y. Cui, X. Chang, X. Zou, Z. Li, Selective solid-phase extraction of lead(II) from biological and natural water samples using surface-grafted lead(II)-imprinted polymers, Microchim. Acta 164 (2009) 125–132.
[24] C. Li, J. Gao, J. Pan, Z. Zhang, Y. Yan, Synthesis, characterization, and adsorption performance of Pb (II)-imprinted polymer in nano-TiO_2 matrix, J. Environ. Sci.-China 21 (2009) 1722–1729.
[25] Y. Liu, Z. Liu, J. Gao, J. Dai, J. Han, Y. Wang, J. Xie, Y. Yan, Selective adsorption behavior of Pb(II) by mesoporous silica SBA-15-supported Pb(II)-imprinted polymer based on surface molecularly imprinting technique, J. Hazard. Mater. 186 (2011) 197–205.
[26] R.A. Garcia-Delgado, L.M. Cotoruelo-Minguez, J.J. Rodriguez, Equilibrium Study of Single-Solute Adsorption of Anionic Surfactants with Polymeric XAD Resins, Sep. Sci. Technol. 27 (1992) 975–987.
[27] A. Hosseini-Bandegharaei, M. Karimzadeh, M. Sarwghadi, A. Heydarbeigi, S.H. Hosseini, M. Nedaie, H. Shoghi, Use of a selective extractant-impregnated resin for removal of Pb(II) ion from waters and wastewaters: Kinetics, equilibrium and thermodynamic study, Chem. Eng. Res. Des. 92 (2014) 581–591.